Proceedings of DSCC2008
2008 ASME Dynamic Systems and Control Conference
October 20-22, 2008, Ann Arbor, Michigan, USA

DSCC2008-2182

ADAPTIVE ROBUST CONTROL OF A LINEAR MOTOR DRIVEN PRECISION INDUSTRIAL GANTRY WITH IMPROVED COGGING FORCE COMPENSATION *

LU LU
SKOFPTC †
ZHEJIANG UNIVERSITY
HANGZHOU, ZHEJIANG, 310027, CHINA
EMAIL: *LULU.LVLV@GMAIL.COM*

BIN YAO
SCHOOL OF MECHANICAL ENGINEERING
PURDUE UNIVERSITY, WEST LAFAYETTE, IN 47907
EMAIL: *BYAO@PURDUE.EDU*
KUANG-PIU PROFESSOR, SKOFPTC
ZHEJIANG UNIVERSITY, HANGZHOU, 310027, CHINA

ZHENG CHEN
SKOFPTC
ZHEJIANG UNIVERSITY
HANGZHOU, ZHEJIANG, 310027, CHINA
EMAIL: *CWLINUS@GMAIL.COM*

QINGFENG WANG
SKOFPTC
ZHEJIANG UNIVERSITY
HANGZHOU, 310027, CHINA
EMAIL: *QFWANG@ZJU.EDU.CN*

ABSTRACT

This paper proposes a new model for cogging forces of linear motor systems. Sinusoidal functions of positions are used to capture the largely periodic nature of cogging forces with respect to position effectively while B-spline functions are employed to account for the additional aperiodic part of cogging forces. This model is experimentally demonstrated to be able to capture both the periodic and non-periodic characteristics of cogging force while having a linear parametrization form which makes effective on-line adaptive compensation of cogging forces possible. A discontinuous projection based desired compensation adaptive robust controller (DCARC) is then constructed for linear motors, which makes full use of the proposed cogging force model for an improved cogging force compensation. Comparative experimental results are obtained on both axes of a linear motor driven Anorad industrial gantry having a linear encoder resolution of 0.5 μm. Experiments are done with each axis running separately to compare the three algorithms: DCARC without cogging force compensation, DCARC with sinusoidal cogging force model compensation, and DCARC with the proposed cogging force model compensation. The results show that DCARC with proposed model compensation achieves the best tracking performance among the three algorithms tested, validating the proposed cogging force model. The excellent tracking performances obtained in experiments also verify the effectiveness of the proposed ARC control algorithms in practical applications.

*THE WORK IS SUPPORTED IN PART BY THE US NATIONAL SCIENCE FOUNDATION (GRANT NO. CMS-0600516) AND IN PART BY THE NATIONAL NATURAL SCIENCE FOUNDATION OF CHINA (NSFC) UNDER THE JOINT RESEARCH FUND FOR OVERSEAS CHINESE YOUNG SCHOLARS(GRANT NO. 50528505)

† THE STATE KEY LABORATORY OF FLUID POWER TRANSMISSION AND CONTROL

INTRODUCTION

The problem of linear motor controls has received significant attentions in recent researches [1–5]. In controlling iron-core linear motors with permanent magnets, cogging forces, which arise due to the strong attraction forces between the iron-core and the permanent magnets, is a common phenomenon that cannot be ignored [4]. The control performances may deteriorate in presence of cogging forces when they are not appropriately accounted for. Thus significant research efforts have been devoted to the modeling and compensation of cogging forces [4, 6–9]. In [4], feedforward compensation terms, which are based on an off-line experimentally identified model of first-order approximation of cogging forces, are added to the position controller. Since not all magnets in a linear motor and not all linear motors

of the same type are identical, feedforward compensation based on off-line identification model may be too sensitive and costly to be useful. In [6–8], the cogging force is assumed to be periodic functions with respect to position. Thus, Fourier expansion has been utilized, with the choice of first few significant terms, to represent the cogging force. Based on this, compensation algorithms have been designed and implemented. In another type of research such as [9], a neural-network-based learning feedforward controller is proposed to reduce positional inaccuracy due to cogging forces or any other reproducible and slowly varying disturbances. But this method simply assumes cogging force to be a general nonlinear function with respect to position, without considering its periodic nature. Furthermore, overall closed-loop stability is not guaranteed. In fact, it is observed in [9] that instability may occur at high-speed movements.

Cogging forces have periodic nature, but due to the complicated physical interactions between different magnets, they may show some aperiodic characteristics. In this paper, we conduct explicit measurement of cogging forces on both axes of a linear motor driven Anorad industrial gantry. The measured cogging forces exhibit certain periodic characteristics with respect to position, which can be represented by sinusoidal functions of positions with unknown weights. However, the amplitude of the weights changes significantly with position, as can be observed from the measurement. Based on this observation, a new model is proposed, considering both the periodic and non-periodic characteristics of cogging forces. We use sinusoidal functions of position to be part of basis functions. B-spline functions are then constructed to capture the changing amplitudes of sinusoidal functions with respect to position. The proposed model is demonstrated experimentally to be able to approximate the measured cogging forces very well, by using a least-squares curve fitting method.

As opposed to the traditional neural-network-based blind modeling of cogging forces [9], the compactness and the linear-parametrization form of the proposed model makes it a perfect choice for on-line adaptive cogging force compensation as well. To this end, a suitable model-based compensation algorithm should be designed. The idea of adaptive robust control (ARC) [10, 11] incorporates the merits of deterministic robust control (DRC) and adaptive control (AC), which guarantees certain robust performance in presence of uncertainties while having a controlled robust learning process for better control performance. The ARC has been extended into the desired compensation ARC (DCARC) in [12].

On the second half of this paper, a DCARC algorithm is designed making full use of the proposed cogging force model. The algorithm is then tested on a two-axes iron-core linear motor driven industrial gantry with severe cogging force effect. Comparative experimental results with each axis running separately show an improved performance over the previously obtained results with DCARCs [13] for both axes after using the proposed cogging force model, though the two axes have different measured cogging force patterns which are assumed to be unknown to users in the controller designs. These results validate the usefulness of the proposed cogging force model for linear motor controls and the excellent tracking performance of the proposed DCARC in practical applications.

MODELING OF SYSTEMS AND PROBLEM FORMULATION

The dynamics of 1-DOF linear motor systems can be represented by the following equation [14, 15]:

$$M\ddot{x} + B\dot{x} + F_c(\dot{x}) + F_r(x) = u + d \tag{1}$$

where x represents the position of linear motor, with its velocity and acceleration denoted as $\dot{x}$ and $\ddot{x}$ respectively. M and B are the mass and viscous friction coefficient, respectively. $F_c(\dot{x})$ is the Coulomb friction term which is modeled by :

$$S_f(\dot{x}) = A_f S_f(\dot{x}) \tag{2}$$

where A_f represents the unknown Coulomb friction coefficient and $S_f(\dot{x})$ is a known continuous or smooth function used to approximate the traditional discontinuous sign function $\mathrm{sgn}(\dot{x})$ for effective friction compensation in implementation. In Eq. (1), $F_r(x)$ represents the position dependent cogging force. u is the control input force. d represents the lumped effect of external disturbances and various types of modeling errors.

Traditionally, cogging forces are assumed to be continuous periodic functions with respect to position [14]. As a result, it can be represented by $F_r(x) = \sum_{i=1}^{\infty}(S_i \sin(\frac{2i\pi}{P}x) + C_i \cos(\frac{2i\pi}{P}x))$ where P is the pitch of magnet pairs and S_i and C_i are some constants. Practically, we can select the first few important terms and ignore all higher terms, i.e. i is from 0 to a positive integer n. This equation can well explain the periodic phenomena of cogging force and has been widely used in compensation algorithms [6–8, 13].

However, due to many complicated physical effects, such as the differences among magnets, the actual cogging force may not be exactly periodic. In the experimental section of this paper, we measure the cogging forces explicitly using a force sensor. It can be observed that the amplitudes of sinusoidal functions vary with the change of position. Thus, using the periodic assumption may give an inaccurate model of cogging force and may deteriorate the resulting control performance. In order to capture the actual cogging force more precisely to achieve better tracking control performances, it is necessary to assume S_i and C_i to be functions of position, namely $S_i = f_{Si}(x)$ and $C_i = f_{Ci}(x)$. With such a varying amplitude modification to periodic functions, the cogging force model becomes:

$$F_r(x) = \sum_{i=1}^{n}(f_{Si}(x) \sin(\frac{2i\pi}{P}x) + f_{Ci}(x) \cos(\frac{2i\pi}{P}x)) \tag{3}$$

The selection of f_{Sin} and f_{Cin} should also make full use of available physical characteristics of cogging forces to ease the design of effective on-line adaptive cogging force compensation. To this end, B-spline functions [16] are utilized to give a mathematical model of f_{Si} and f_{Ci} respectively. Namely, f_{Si} and f_{Ci} are chosen as:

$$f_{Si}(x) = \sum_{j=1}^{m} N_{j,k}(x) S_{ij} \tag{4}$$

$$f_{Ci}(x) = \sum_{j=1}^{m} N_{j,k}(x) C_{ij} \tag{5}$$

where

$$\begin{cases} N_{j,k}(x) = \begin{cases} 1 & \text{when } x \in [X_j,\, X_{j+1}) \\ 0 & \text{else} \end{cases} & k = 1 \\ N_{j,k}(x) = \frac{x - X_j}{X_{j+k-1} - X_j} N_{j,k-1}(x) + \frac{X_{j+k} - x}{X_{j+k} - X_{j+1}} N_{j+1,k-1}(x) & k \geq 2 \end{cases} \tag{6}$$

where k is the order of B-spline and m is the number of control points needed. $[X_1, X_2, \cdots, X_{m+k-1}, X_{m+k}]$ is the knot vector, with $X_{j+1} \geq X_j$ defined to be as follows. Let m be the number of magnet segments on the linear motor axis. If a kth order B-spline function is used, then X_k is defined to be the position of the first magnet and X_{k+m} the last magnet, with X_{k+j} as the position of the $j+1$-th magnet. By the construction of linear motor, $X_{k+j} = X_k + jP,\ j = 1, \ldots m$. So define $X_1, \cdots, X_{k-1}$ as $X_{k-j} = X_k - jP,\ j = 1, \ldots k-1$. Fig. 1 illustrates the linear motor position x on the range defined by knot vector. Assuming a linear motor of 5 magnet segments, the shapes of $f_{Si}(x)$ for the order of $k = 1, 3$ with the values of control points described by the green dots are shown in Figs. 2 to 3 respectively.

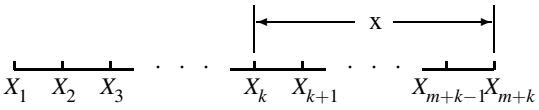

Figure 1. Illustration of Linear Motor Position Range on B-Spline Interval

Using B-spline function has the following merits:

1: The increment of neighboring elements in knot vector of B-spline function is selected as the physical pitch of magnets on the linear motor axis, i.e., $X_{j+1} - X_j = P$. This means that the value of B-spline function changes with a unit of magnets' pitch. Physically, it can interpret the changing amplitude of sinusoidal function caused by difference of each magnet.

2: B-spline function is linear to the control points (S_{ij} and C_{ij}). The resulting cogging force model described by Eqs. (3) to (4) is thus linearly parametrized by the control points (S_{ij} and C_{ij}) with known basis functions. Such a model significantly simplifies the on-line estimate of unknown control points for adaptive compensation of cogging forces.

3: The basis function $N_{j,k}(x)$ is only active when $x \in [X_j, X_{j+k})$ and is zero in other regions. Such a nice property is especially preferable for real-time adaptive controls because in every sampling period, we only have to fetch a small portion of parameter estimates from memory for compensation and update. For example, when $x \in [X_l, X_{l+1})$ for some l, only $S_{i(l-k+1)}$, $C_{i(l-k+1)}$, $\cdots$, S_{il}, C_{il} are needed for update and compensation. All other coefficients need not be considered. Thus the algorithm is economic, especially when k is chosen small.

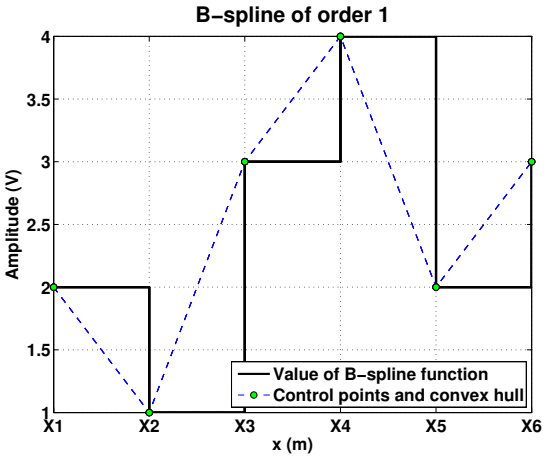

Figure 2. B-Spline of Order 1

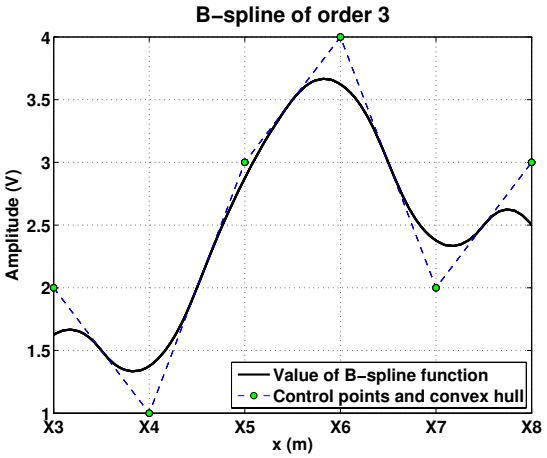

Figure 3. B-Spline of Order 3

Combining Eqs. (3) - (5), the cogging force $F_r(x)$ is put in a concise form as:

$$F_r(x) = A_r^T S_r(x) \tag{7}$$

where $A_r = [S_{11},\ C_{11},\ ...,\ S_{ji},\ C_{ji},\ ...,\ S_{mn},\ C_{mn}]^T \in R^{2mn}$ is the vector of unknown control points and

$$S_r = [N_{1,k}(x)\sin(\frac{2\pi}{P}x),\ N_{1,k}(x)\cos(\frac{2\pi}{P}x),\ ...,\ N_{j,k}(x)\sin(\frac{2i\pi}{P}x),\ N_{j,k}(x)\cos(\frac{2i\pi}{P}x),\ ...,\ N_{m,k}(x)\sin(\frac{2n\pi}{P}x),\ N_{m,k}(x)\cos(\frac{2n\pi}{P}x)]^T$$

is a vector of known basis functions. With this cogging force model, the linear motor dynamics (1) can be linear parameterized as:

$$M\ddot{x} + B\dot{x} + A_f S_f(\dot{x}) + A_r^T S_r(x) - d_n = u + \tilde{d} \tag{8}$$

where d_n denotes the nominal value of d and $\tilde{d} = d - d_n$ represents the time-varying portion of the lumped uncertainties. (8) can also be put in a state space form of

$$\dot{x}_1 = x_2 \tag{9}$$

$$M\dot{x}_2 = u - Bx_2 - A_f S_f(x_2) - A_r^T S_r(x_1) + d_n + \tilde{d} \tag{10}$$

where x_1 and x_2 are the position and velocity respectively.

Let $x_d(t)$ be the desired motion trajectory, which is assumed to be known, bounded with bounded derivatives up to the second order. The objective is to synthesize a bounded control input u such that the output x_1 tracks $x_d(t)$ as closely as possible in spite of various modeling uncertainties.

ADAPTIVE ROBUST CONTROL (ARC)

Assumptions

The left hand side of equation Eq. (8) is the sum of known functions times unknown parameters. Let us denote the unknown parameter set as $\theta = [M,\ B,\ A_f,\ A_r^T,\ -d_n]^T \in R^{4+2mn}$, with $\theta_1 = M$, $\theta_2 = B$, $\theta_3 = A_f$, $\theta_{4b} = A_r$, $\theta_5 = -d_n$. In order to design bounded control law with guaranteed transient performance, the following practical assumption on parametric uncertainties is made:

Assumption 1. *The extent of the parametric uncertainties and uncertain nonlinearities are known, i.e.,*

$$\theta \in \Omega_\theta \triangleq \{\ \theta :\ \ \theta_{min} < \theta < \theta_{max}\ \} \tag{11}$$

$$\tilde{d} \in \Omega_d \triangleq \{\ \tilde{d} :\ \ |\tilde{d}| \le \delta_d\ \} \tag{12}$$

where $\theta_{min} = [\theta_{1min},\ \cdots,\ \theta_{(4+2mn)min}]^T$, $\theta_{max} = [\theta_{1max},\ \cdots,\ \theta_{(4+2mn)max}]^T$, *and* δ_d *are known.* ◇

Notations and Discontinuous Projection

Let $\hat{\theta}$ denote the estimate of θ and $\tilde{\theta}$ the estimation error (i.e., $\tilde{\theta} = \hat{\theta} - \theta$). In view of Eq. (11), the following discontinuous projection type adaptation law will be used

$$\dot{\hat{\theta}} = Proj_{\hat{\theta}}(\Gamma\tau) \tag{13}$$

where $\Gamma > 0$ is a diagonal matrix, τ is an adaptation function to be synthesized later. The projection mapping $Proj_{\hat{\theta}}(\bullet) = [Proj_{\hat{\theta}_1}(\bullet_1), \cdots, Proj_{\hat{\theta}_5}(\bullet_5)]^T$ is defined in element as

$$Proj_{\hat{\theta}_i}(\bullet_i) = \begin{cases} 0 & \text{if } \hat{\theta}_i = \theta_{imax} \text{ and } \bullet_i > 0 \\ 0 & \text{if } \hat{\theta}_i = \theta_{imin} \text{ and } \bullet_i < 0 \\ \bullet_i & \text{otherwise} \end{cases} \tag{14}$$

Adaptive Robust Control (ARC) Law Synthesis

Define a switching-function-like quantity p as:

$$p \triangleq \dot{e} + k_1 e = x_2 - x_{2eq}, \quad x_{2eq} \triangleq \dot{x}_d - k_1 e, \tag{15}$$

where $e = x_1 - x_d(t)$ is the output tracking error and $k_1 > 0$ is a positive gain. If p is small or converges to zero, then the output tracking error e will be small or converge to zero since $G_p(s) = \frac{e(s)}{p(s)} = \frac{1}{s+k_1}$ is a stable transfer function. So the rest of the design is to make p as small as possible. Differentiating (15) and noting Eq. (10), one obtains

$$\begin{aligned} M\dot{p} &= u - \theta_1\dot{x}_{2eq} - \theta_2 x_2 - \theta_3 S_f - \theta_{4b}^T S_r - \theta_5 + \tilde{d}, \\ &= u + \varphi^T\theta + \tilde{d} \end{aligned} \tag{16}$$

where $\dot{x}_{2eq} = \Delta = \ddot{x}_d - k_1\dot{e}$ and $\varphi^T = [-\dot{x}_{2eq},\ -x_2,\ -S_f(x_2),\ -S_r(x_1),\ -1]$. We propose the following ARC control law:

$$u = u_a + u_s,\ \ u_a = -\varphi^T\hat{\theta}, \tag{17}$$

where u_a is the adjustable model compensation needed for perfect tracking, and u_s is a robust control law to be synthesized later. Substituting Eq. (17) into Eq. (16), and then simplifying the resulting expression, one obtains

$$M\dot{p} = u_s - \varphi^T\tilde{\theta} + \tilde{d}. \tag{18}$$

The robust control function u_s has the following structure:

$$u_s = u_{s1} + u_{s2}, \quad u_{s1} = -k_{s1}p, \tag{19}$$

where u_{s1} is a simple proportional feedback to stabilize the nominal system and u_{s2} is a robust performance feedback term having the following properties [11]:

$$\begin{array}{c} p\{u_{s2} - \varphi^T \tilde{\theta} + \tilde{d}\} \leq \varepsilon \\ p u_{s2} \leq 0 \end{array} \tag{20}$$

where ε is a design parameter that can be arbitrarily small. The exact forms of u_{s2} satisfying the above properties can be found in [11]. With the proposed control law, we have the following theorem.

Theorem 1. *If the adaptation function in Eq. (13) is chosen as*

$$\tau = \varphi p, \tag{21}$$

then the ARC control law Eq. (17) guarantees that [14]:

A. *In general, all signals are bounded. Furthermore, the positive definite function V_s defined by*

$$V_s = \frac{1}{2} M p^2 \tag{22}$$

is bounded above by

$$V_s \leq \exp(-\lambda t) V_s(0) + \frac{\varepsilon}{\lambda}[1 - \exp(-\lambda t)], \tag{23}$$

where $\lambda = 2k_{s1}/\theta_{1max}$.

B. *If after a finite time t_0, there exist parametric uncertainties only (i.e., $\tilde{d} = 0$, $\forall t \geq t_0$), then, in addition to results in A, zero final tracking error is also achieved, i.e, $e \longrightarrow 0$ and $p \longrightarrow 0$ as $t \longrightarrow \infty$.*

Desired Compensation Adaptive Robust Control (DCARC)

DCARC uses desired trajectory signals to form regressor, which has been shown to outperform ARC in terms of all indexes [15]. Following the same design procedure as in [13], a DCARC law using the proposed cogging force model is also constructed as follows:

By applying the Mean Value Theorem, we have

$$S_f(x_2) - S_f(\dot{x_d}) = g_f(x_2, t)\dot{e} \tag{24}$$

$$S_r(x_1) - S_r(x_d) = g_r(x_1, t)e \tag{25}$$

where $g_f(x_2, t)$ and $g_r(x_1, t)$ are certain nonlinear functions. The control law is thus given by:

$$u = u_a + u_s,\ u_a = -\varphi_d^T \hat{\theta} \tag{26}$$

$$u_s = u_{s1} + u_{s2},\ u_{s1} = -k_{s1} p \tag{27}$$

$$\dot{\hat{\theta}} = Proj_{\hat{\theta}}(\Gamma \varphi_d p) \tag{28}$$

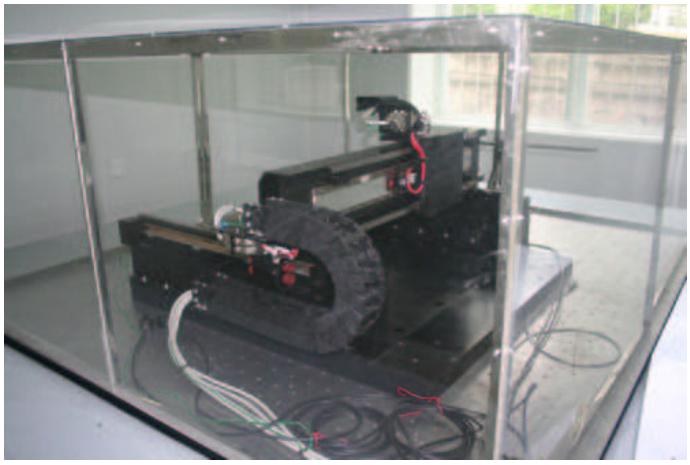

Figure 4. Gantry Type Linear Motor Drive System

where $\varphi_d^T = [-\ddot{x}_d, -\dot{x}_{1d}, -S_f(\dot{x}_d), -S_r(x_d), -1]$ is the regressor using the desired trajectory signals. k_{s1} is a nonlinear gain large enough such that the matrix below is positive definite

$$\begin{bmatrix} k_{s1} - \theta_1 k_1 + \theta_2 + \theta_3 g_f & -\frac{1}{2}(k_1\theta_2 + k_1\theta_3 g_f - \theta_{4b}^T g_r) \\ -\frac{1}{2}(k_1\theta_2 + k_1\theta_3 g_f - \theta_{4b}^T g_r) & \frac{1}{2} M k_1^3 \end{bmatrix} \tag{29}$$

u_{s2} is a robust feedback term satisfying

$$\begin{array}{c} p\{u_{s2} - \varphi_d^T \tilde{\theta} + \tilde{d}\} \leq \varepsilon \\ p u_{s2} \leq 0 \end{array} \tag{30}$$

where ε is a design parameter that can be arbitrarily small. It can be proved using the same technique as in [15] that the results like Theorem 1 still hold. Due to the page limits, the details are omitted and can be obtained from the authors.

EXPERIMENTAL RESULTS

Experimental Setup

In the Precision Mechatronics Laboratory at Zhejiang University, a two-axes commercial Anorad HERC-510-510-AA1-B-CC2 Gantry by Rockwell Automation has been set up, as shown in Fig.4. Both axes of the gantry are powered by Anorad LC-50-200 iron core linear motors and have a travel distance of 0.51 m. Linear encoders provide both axes a position measurement resolution of $0.5\mu m$. To implement real-time control algorithm, the above system is connected to a dSPACE DS1103 controller board.

System Identification

Experiments have been conducted on the X-axis and Y-axis separately. Off-line parameter identification is first carried out and it is found that nominal values of the system parameters

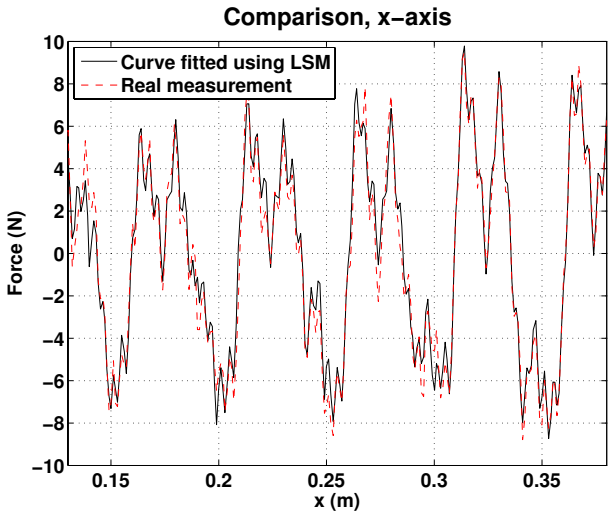

Figure 5. Measured Cogging Forces of X-Axis And Its Curve Fitting

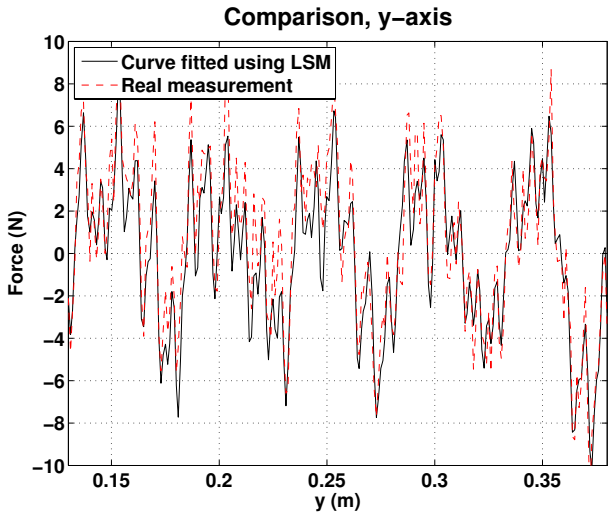

Figure 6. Measured Cogging Forces of Y-Axis And Its Curve Fitting

without loads are $M = 0.12 volt/m/sec^2$, $B = 0.166 volt/m/sec$, $A_f = 0.15 volt$ for X-axis, and $M = 0.64 volt/m/sec^2$, $B = 0.24 volt/m/sec$, $A_f = 0.66 volt$ for Y-axis, in which all values shown are normalized with respect to the input voltage in terms of *volt* sent to the linear motors.

Explicit measurement of cogging force is then conducted for both axes by blocking the motor and using an external force sensor to measure the blocking forces at zero input voltages. This measurement is done for various positions with $1mm$ incremental distance. The measured cogging forces are shown in Fig. 5 for X-axis, and Fig. 6 for Y-axis respectively. As can be seen from the figures, both axes of cogging forces have periodic characteristics with respect to position, with the fundamental period corresponding to the pitch of the magnets ($P = 50mm$). However, it is also observed that the amplitude of this largely periodic function vary significantly in the travel range.

The method proposed in this paper is then used to approximate the measured cogging forces. After applying FFT to Fig. 5 and 6, it is observed that the harmonic terms of cogging forces for both axes have significant values at frequencies corresponding to $i = 1, 2, 3, 6, 12$ in (3). So these five frequencies are kept when approximating cogging forces. Third order B-spline functions are used to capture the change of amplitudes of cogging forces during the travel range. A curve fitting using the standard Least Square Method (LSM) is then performed to obtain the values of B-spline control points in (7) that best approximate the measured cogging forces. The output of the resulting cogging force models are plotted against the measured ones in Fig. 5 for X-axis and in Fig. 6 for Y-axis respectively. As can be seen from the figures, the proposed cogging force model well captures the largely periodic nature as well as the changing amplitude of cogging force with respect to position.

Comparative Experimental Results for X-axis

For X-axis, the dSPACE controller's sampling frequency is selected as $f_s = 5kHz$, which results in a velocity measurement resolution of $0.0025\ m/sec$ for the linear encoder feedback. The following three control algorithms are compared:

C1: DCARC without cogging force compensation.
C2: DCARC with cogging force compensation based on periodic cogging force models [6, 13].
C3: DCARC with cogging force compensation based on the proposed model.

To have a fair comparison, all the controller parameters of the above three algorithms are chosen the same when they have the same meaning. Namely, the lower and upper bounds of the parameter variations for M, B, A_f, d for X-axis are chosen as $[0.1,\ 0.15,\ 0.1,\ -0.5]$ and $[0.2,\ 0.35,\ 0.3,\ 0.5]$, respectively. The upper and lower bounds of coefficients in A_r in both the algorithms C2 and C3 are set as 0.1 and -0.1 respectively. For all control algorithms, the feedback gains are set at $k_1 = 200$ and $k_{s1} = 400 * 0.12$ with the adaptation gains for M, B, A_f, d chosen as $[1,\ 10,\ 10,\ 1000]$. The adaptation gains for all coefficients in A_r are chosen as 100. For the algorithm C3, third order B-spline along with the first three harmonic frequencies ($i = 1, 2, 3$) are used for the on-line cogging force compensation model.

The desired trajectory used represents point-to-point movements, typical in manufacture industry, with a travel distance of $0.4m$, a maximum velocity of $0.5m/sec$ and a maximum acceleration of $10m/sec^2$. Fig. 7 shows the tracking error of three algorithms, with the magnified plot over a single running period shown in Fig. 8. From these error plots, it is observed that the tracking errors are quite different during the constant speed motion period. Namely, with the periodic cogging force compensation, the tracking error is substantially reduced in DCARC C2

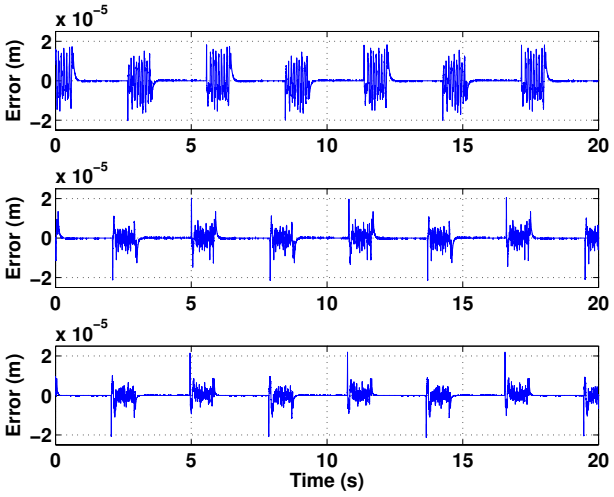

Figure 7. Comparison of Tracking Errors, X-Axis

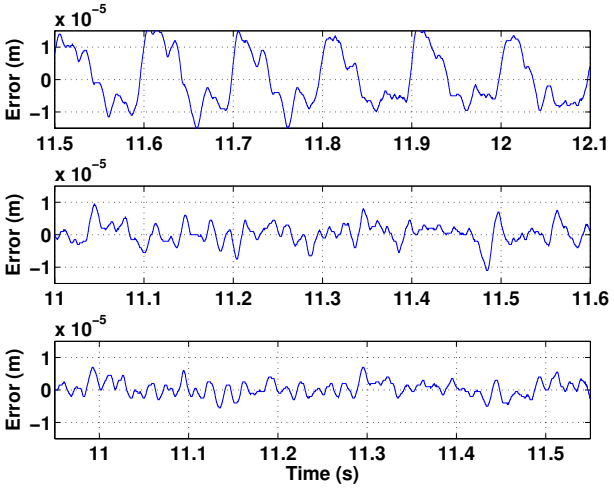

Figure 8. Magnification in One Running Period

when compared to DCARC C1 with no cogging force compensation. The tracking error is further reduced with the proposed cogging force compensation, with the cogging force shape of tracking error plot no longer evident revealing a smoother constant speed movement. Tab. 1 shows the performance indexes for the three algorithms. It is also evident from these quantitative measures that the proposed algorithm outperforms the other two.

Comparative Experimental Results for Y-axis

The above three DCARC algorithms are also tested and compared on Y-axis of the Anorad gantry, which has a quite different measured cogging force pattern than that of X-axis. The sampling frequency is also selected as $f_s = 5kHz$. In all the three algorithms, the lower and upper bounds of the parameter variations for M, B, A_f, d are chosen as $[0.5,\ 0.1,\ 0.3,\ -0.8]$ and

Table 1. Performance Index, X-Axis.

Algorithms	$\|e\|_\infty\ (m)$	$\|e\|_2\ (m)$
C1	1.6500e-005	8.3408e-006
C2	1.1000e-005	3.1064e-006
C3	6.9996e-006	2.3043e-006

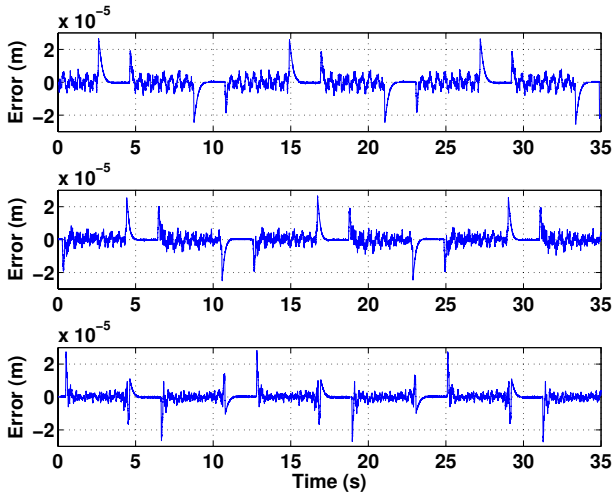

Figure 9. Comparison of Tracking Errors in Normal Speed, Y-Axis

$[0.75,\ 0.3,\ 0.8,\ 0.8]$, respectively. As to A_r, we select all the upper bounds of its coefficients as 0.2, and lower bounds as -0.2, for both algorithms C2 and C3. $k_1 = 100$ and $k_{s1} = 150 * 0.64$ for all algorithms. The adaptation gains for M, B, A_f, d are chosen as $[1,\ 10,\ 10,\ 1000]$. The adaptation gains for coefficients in A_r are 100. For algorithm C3, third order B-spline with three harmonic frequencies $(i = 1, 6, 12)$ are used for cogging force compensation. A desired trajectory with $0.1m/sec$ as the maximum velocity and $1m/sec^2$ as the maximum acceleration is used in all experiments.

Fig. 9 shows the tracking error of three algorithms with the magnified plot of errors over a single running period shown in Fig. 10. As seen from these figures, the tracking error is reduced a little bit after using algorithm C2. But the shape of cogging force is still evident in the tracking error plot. However, such a shape cannot be observed in the tracking error plot with algorithm C3 anymore, indicating a smoother constant speed motion. Tab. 2 shows the performance indexes for the three algorithms. Again, a significantly improved control performance is seen for the proposed algorithm C3. All these results demonstrate the effectiveness of the proposed cogging force compensation in practical applications.

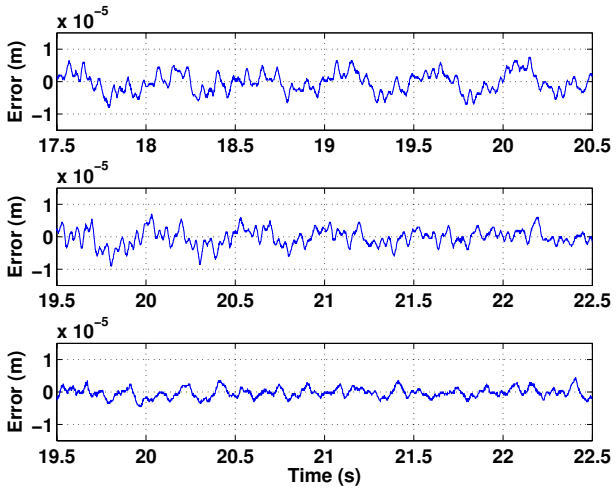

Figure 10. Magnification in One Running Period

Table 2. Performance Index, Y-Axis.

Algorithms	$\|e\|_\infty$ (m)	$\|e\|_2$ (m)
C1	8.0002e-006	3.0642e-006
C2	9.0003e-006	2.5790e-006
C3	4.5002e-006	1.5096e-006

CONCLUSION

In this paper, a new cogging force model capable of capturing both the periodic and non-periodic characteristics of cogging forces is proposed. The linearly parameterized form and the computational efficiency of the model also lends itself an ideal choice for on-line adaptive cogging force compensation. Adaptive robust control algorithms making full use of the proposed cogging force model are also developed for linear motor controls. The proposed algorithms have been implemented on a linear motor driven two-axes commercial gantry system. Comparative results show that smaller tracking error and smoother constant speed motion are obtained using ARC with the proposed cogging force compensation than the ones with periodic cogging force compensation, demonstrating the effectiveness of the proposed algorithms in practical applications.

REFERENCES

[1] Alter, D. M., and Tsao, T. C., 1996. "Control of linear motors for machine tool feed drives: design and implementation of h_∞ optimal feedback control". *ASME J. of Dynamic systems, Measurement, and Control,* **118**, pp. 649–656.

[2] Komada, S., Ishida, M., Ohnishi, K., and Hori, T., 1991. "Disturbance observer-based motion control of direct drive motors". *IEEE Transactions on Energy Conversion,* **6**(3), pp. 553–559.

[3] Egami, T., and Tsuchiya, T., 1995. "Disturbance suppression control with preview action of linear dc brushless motor". *IEEE Transactions on Industrial Electronics,* **42**(5), pp. 494–500.

[4] Braembussche, P. V., Swevers, J., Brussel, H. V., and Vanherck, P., 1996. "Accurate tracking control of linear synchronous motor machine tool axes". *Mechatronics,* **6**(5), pp. 507–521.

[5] Hong, Y., and Yao, B., 2007. "A globally stable high performance adaptive robust control algorithm with input saturation for precision motion control of linear motor drive system". *IEEE/ASME Transactions on Mechatronics,* **12**(2), pp. 198–207. Part of the paper appeared in the *IEEE/ASME Conference on Advanced Intelligent Mechatronics (AIM'05)*, pp.1623-1628, 2005.

[6] Xu, L., and Yao, B., 2000. "Adaptive robust precision motion control of linear motors with ripple force compensation: Theory and experiments". In Proc. of IEEE Conference on Control Applications, pp. 373–378. (Winner of the Best Student Paper Competition).

[7] Roehrig, C., 2005. "Force ripple compensation of linear synchronous motors". *Asian Journal of Control,* **7**(1), March, pp. 1–11.

[8] Hwang, T.-S., Seok, J.-K., and Kim, D.-H., 2006. "Active damping control of linear hybrid stepping motor for cogging force compensation". *IEEE Transactions on Magnetics,* **42**(2), February, pp. 329–334.

[9] Otten, G., Vries, T., Amerongen, J., Rankers, A., and Gaal, E., 1997. "Linear motor motion control using a learning feedforward controller". *IEEE/ASME Transactions on Mechatronics,* **2**(3), pp. 179–187.

[10] Yao, B., and Tomizuka, M., 1996. "Smooth robust adaptive sliding mode control of robot manipulators with guaranteed transient performance". *Trans. of ASME, Journal of Dynamic Systems, Measurement and Control,* **118**(4), pp. 764–775. Part of the paper also appeared in the *Proc. of 1994 American Control Conference*, pp.1176–1180.

[11] Yao, B., and Tomizuka, M., 1997. "Adaptive robust control of SISO nonlinear systems in a semi-strict feedback form". *Automatica,* **33**(5), pp. 893–900. (Part of the paper appeared in Proc. of 1995 American Control Conference, pp2500-2505, Seattle).

[12] Yao, B., 1998. "Desired compensation adaptive robust control". In Proceedings of the ASME Dynamic Systems and Control Division, DSC-Vol.64, IMECE'98, pp. 569–575. The revision will appear in the *ASME J. of Dynamic Systems, Measurement, and Control*.

[13] Yao, B., Hu, C., and Wang, Q., 2007. "Adaptive robust precision motion control of high-speed linear motors with on-line cogging force compensations". In Proceedings of IEEE/ASME Conference on Advanced Intelligent Mechatronics, pp. 1–6.

[14] Yao, B., and Xu, L., 2002. "Adaptive robust control of linear motors for precision manufacturing". *International Journal of Mechatronics,* **12**(4), pp. 595–616. Part of the paper appeared in *The 14th IFAC World Congress, Vol. A* , pp25-30, Beijing, 1999.

[15] Xu, L., and Yao, B., 2001. "Adaptive robust precision motion control of linear motors with negligible electrical dynamics: theory and experiments". *IEEE/ASME Transactions on Mechatronics,* **6**(4), pp. 444–452.

[16] de Boor, C., 2001. *A Practical Guide to Splines*. Springer-Verlag, December.